PNAS
www.pnas.org

Supplementary Information

Renal Control of Disease Tolerance To Malaria

Susana Ramos, Ana Rita Carlos, Balamurugan Sundaram, Viktoria Jeney, Ana Ribeiro, Raffaella Gozzelino, Claudia Bank, Erida Gjini, Faouzi Braza, Rui Martins, Temitope Wilson Ademolue, Birte Blankenhaus, Zélia Gouveia, Pedro Faísca, Damian Trujillo, Sílvia Cardoso, Sofia Rebelo, Laura del Barrio, Abolfazl Zarjou, Subhashini Bolisetty, Anupam Agarwal & Miguel P. Soares

Correspondence: Miguel P. Soares
Email: mpsoares@igc.gulbenkian.pt

This PDF file includes:

www.pnas.org/cgi/doi/10.1073/pnas.1822024116

Detailed Material and Methods

Conditional allele deletions. C57BL/6J mice were obtained from the IGC animal facility. C57BL/6 *Nrf2*$^{-/-}$ mice (1) were obtained originally from the RIKEN BioResource Center (BRC: 01390, Koyadai, Tsukuba, Ibaraki, Japan) and maintained thereafter at the IGC animal facility. Mice were genotyped by PCR.

C57BL/6 *Pepck*$^{Cre/Wt}$ mice (2, 3) were obtained originally from Anupam Agarwal (University of Alabama at Birmingham). *Hmox1* floxed (*Hmox1*$^{fl/fl}$) mice (4) were obtained originally from the Riken BRC experimental animal division (Japan) (http://mus.brc.riken.jp/en/link). *Pepck*$^{Cre/Wt}$ mice were crossed with *Hmox1*$^{fl/fl}$ to generate *Pepck*$^{Cre/Wt}$*Hmox1*$^{fl/fl}$ (*Hmox1*$^{Pepckfl/fl}$) mice and littermate control *Hmox1*$^{fl/fl}$ mice. Conditional deletion of the *Hmox1*$^{fl/fl}$ allele in RPTEC was induced at 8-week after birth by the addition of 0,3M NH_4Cl to drinking water for one week, as described (2, 3). *Hmox1*$^{fl/fl}$ deletion in the kidneys of *Hmox1*$^{PepckΔ/Δ}$ mice was assessed by qRT-PCR. *Hmox1*$^{PepckΔ/Δ}$ mice were used 4 weeks after exposure to acidified water. C57BL/6J *Fth* floxed (*Fth*$^{fl/fl}$)(5) mice were obtained originally from Lukas Kuhn (Ecole Polytechnique Fédérale de Lausanne, Faculté des Sciences de la Vie, Institut Suisse de Recherche Expérimentale sur le Cancer). C57BL/6 *Pepck*$^{Cre/Wt}$ mice (2, 3) were crossed with *Fth*$^{fl/fl}$ to generate *Pepck*$^{Cre/Wt}$*Fth*$^{fl/fl}$ (*Fth*$^{Pepckfl/fl}$) mice and littermate control *Fth*$^{fl/fl}$ mice. Conditional deletion of the *Fth*$^{fl/fl}$ allele in RPTEC was induced at 8-week after birth as described for *Hmox1* deletion. Deletion of the *Fth*$^{fl/fl}$ allele in the kidneys of *Fth*$^{PepckΔ/Δ}$ mice was assessed by qRT-PCR. *Fth*$^{PepckΔ/Δ}$ mice were used 4 weeks after exposure to acidified water.

C57BL/6 *Mx1*$^{Cre/Wt}$ mice were obtained originally from the Jackson Laboratory (B6.Cg-Tg (Mx1-cre)1Cgn/J; #003556)(6) and *Mx1*$^{Cre/Wt}$*Hmox1*$^{fl/fl}$ mice were generated from *Mx1*$^{Cre/Wt}$*Hmox1*$^{fl/fl}$ x *Hmox1*$^{fl/fl}$ breeding. Conditional gene deletion (*Hmox1*$^{Mx1Δ/Δ}$) was achieved in 6-8 weeks old *Hmox1*$^{Mx1fl/fl}$ mice by poly (I:C) (Invivogen, Toulouse, France) administration (i.p.; 1mg/kg body weight, 2x, 3 days apart). *Hmox1* deletion was confirmed by qRT-PCR in whole blood from *Hmox1*$^{Mx1Δ/Δ}$ mice, two weeks after the first poly (I:C) administration. *Hmox1*$^{Mx1Δ/Δ}$ were used 8 weeks after the first poly (I:C) administration. Control *Hmox1*$^{fl/fl}$ littermate mice received poly (I:C) at the same dosage and schedule.

C57BL/6 *R26*^{CreERT2} mice were obtained from the Jackson Laboratory (B6.129-*Gt (ROSA)26Sor*$^{tm1\ (cre/ERT2)Tyj}$/J, #008463)(7). *R26*$^{CreERT2/CreERT2}$*Hmox1*$^{fl/fl}$ (*Hmox1*$^{R26fl/fl}$) mice were obtained from *Hmox1*$^{R26fl/fl}$ x *Hmox1*$^{fl/fl}$ breeding. Conditional gene deletion (*Hmox1*$^{R26Δ/Δ}$) was achieved in 4-5 weeks old mice, fed *ad libitum* with Low

Phytoestrogen Diet (Harlan Laboratories; #2919.CS) for 2 weeks followed by administration of Tamoxifen (Sigma) suspended in sterile corn oil (Sigma) (gavage, 4.5mg per mouse, 1x every second day, 10x). Alternatively, Tamoxifen was provided by *ad libitum* intake of Rat/Mouse diet with Tamoxifen (M-Z, Low phytoestrogen; 360 mg/kg TAM Citrate + Sucrose flavour, 10mm Soybean free diet, sterilized 25 kGy; Ssniff Spezialdiäten GmbH) for 4 weeks. *Hmox1* deletion was assessed by qRT-PCR in whole blood and $Hmox1^{R26\Delta/\Delta}$ mice were used 8 weeks after the last Tamoxifen gavage or 6 weeks after removal of Tamoxifen enriched diet. Control $Hmox1^{fl/fl}$ mice were treated with the same protocol. $Hsf1^{fl/fl}$ mice were obtained originally from Elisabeth Christians (University Pierre et Marie Curie, Paris, France)(8) and were backcrossed into the C57BL/6 background at IGC. C57BL/6 $Hsf1^{fl/fl}$ mice were bred with C57BL/6 $R26^{CreERT2}$ mice (7) to generate $R26^{CreERT2/CreERT2}Hsf1^{fl/fl}$ ($Hsf1^{R26fl/fl}$) mice. These were maintained at the IGC from $Hsf1^{R26fl/fl}$ x $Hsf1^{fl/fl}$ breeding. Conditional gene deletion ($Hsf1^{R26\Delta/\Delta}$) was achieved in 4-5 weeks old mice by Tamoxifen (dissolved in corn oil, 5% Ethanol) administration (gavage, every second day, 3x; 225mg/kg of body weight). *Hsf1* deletion was assessed by qRT-PCR in whole blood from in $Hsf1^{R26\Delta/\Delta}$ mice (>95% deletion). $Hif1\alpha^{fl/fl}$ mice (Jackson Laboratory; B6.129-$Hif1\alpha^{tm3Rsjo/J}$; Stock No: 007561)(9) were bred with C57BL/6 $R26^{CreERT2}$ mice (7) to generate $R26^{CreERT2/CreERT2}Hif1\alpha^{fl/fl}$ ($Hif1\alpha^{R26fl/fl}$) mice. These were maintained at the IGC from $Hif1\alpha^{R26fl/fl}$ x $Hif1\alpha^{fl/fl}$ breeding. Conditional gene deletion ($Hif1\alpha^{R26\Delta/\Delta}$) was achieved and confirmed, as described for $Hsf1^{R26\Delta/\Delta}$ mice (>95% deletion).

C57BL/6 $LysM^{Cre/Cre}Hmox1^{\Delta/\Delta}$ ($Hmox1^{LysM1\Delta/\Delta}$) mice were generated and assessed for *Hmox1* deletion, essentially as described elsewhere (10). C57BL/6 $LysM^{Cre/Cre}Fth^{\Delta/\Delta}$ ($Fth^{LysM\Delta/\Delta}$) mice were generated, as described above for $Hmox1^{LysM\Delta/\Delta}$ and deletion of the *Fth* allele was assessed, essentially as described elsewhere (10).

C57BL/6 $Cd11c^{Cre/Wt}$ were obtained from the Jackson Laboratory (B6.Cg-Tg (Itgax-cre)1-1Reiz/J, #008068)(11) and $Cd11c^{Cre/Wt}Hmox1^{\Delta/\Delta}$ ($Hmox1^{Cd11c\Delta/\Delta}$) mice were obtained from $Hmox1^{Cd11c\Delta/\Delta}$ x $Hmox1^{fl/fl}$ breeding. $Hmox1^{fl/fl}$ littermates were used as controls. *Hmox1* deletion in $Hmox1^{Cd11c\Delta/\Delta}$ mice was assessed by qRT-PCR in $CD11c^{+}$ cells isolated from spleens and purified using anti-$CD11c^{+}$ microbeads (MACS®; Miltenyi Biotec) followed by fluorescence activated cell sorting (FACS) in a MoFlo cell sorter (Beackam Coulter), based on $CD11c^{+}$ and $MHCII^{+}$ and $TCR\alpha/\beta^{-}$, IgM^{-} and $CD19^{-}$ expression.

C57BL/6 *Alb*$^{Cre/Wt}$ were obtained from the Jackson Laboratory (B6.Cg-Tg (Alb-cre)21Mgn/J, #003574)(12) and *Alb*$^{Cre/Wt}$*Fth*$^{\Delta/\Delta}$ (*Fth*$^{Alb\Delta/\Delta}$) mice were generated from *Fth*$^{Alb\Delta/\Delta}$ x *Fth*$^{fl/fl}$ breeding. *Fth*$^{fl/fl}$ littermates were used as controls. Deletion of the *Fth* allele was assessed in the liver, by qRT-PCR, as described elsewhere (13).

C57BL/6 *Tie2*$^{Cre/Wt}$ were obtained from the Jackson Laboratory (B6.Cg-Tg (Tek-cre)1Ywa/J, #008863)(14). *Tie2*$^{Cre/Wt}$*Hmox1*$^{\Delta/\Delta}$ (*Hmox1*$^{Tie2\Delta/\Delta}$) mice were generated from *Hmox1*$^{Tie2\Delta/\Delta}$ x *Hmox1*$^{fl/fl}$ breeding and *Hmox1*$^{fl/fl}$ littermates were used as controls. *Hmox1* deletion was assessed by qRT-PCR in heart-derived endothelial cells purified using CD31 Microbeads (MACS® Technology; Miltenyi Biotec) and in the spleen.

C57BL/6 *Nestin*$^{Cre/Wt}$ mice were obtained originally from the Jackson Laboratory (B6.Cg-Tg (Nes-cre)1Kln/J, #003771)(15). *Nestin*$^{Cre/Wt}$*Hmox1*$^{\Delta/\Delta}$ (*Hmox1*$^{Nestin\Delta/\Delta}$) mice were generated from *Hmox1*$^{Nestin\Delta/\Delta}$ x *Hmox1*$^{fl/fl}$ breeding. *Hmox1*$^{fl/fl}$ littermate mice were used as controls. *Hmox1* deletion was assessed by qRT-PCR in the brain and spinal cord.

C57BL/6 *Cdh5*$^{CreERT2/Wt}$ mice (16) were obtained originally from Prof Ralf H. Adams (Max Planck Institute for Molecular Biomedicine, Münster, Germany). *Cdh5*$^{CreERT2/Wt}$*Fth*$^{fl/fl}$ (*Fth*$^{Cdh5fl/fl}$) mice were generated from *Fth*$^{Cdh5fl/fl}$ x *Fth*$^{fl/fl}$ breeding and *Fth*$^{fl/fl}$ littermates were used as controls. Conditional deletion of the *Fth* allele (*Fth*$^{Cdh5\Delta/\Delta}$) was induced in 6-week old *Fth*$^{Cdh5fl/fl}$ mice by Tamoxifen administration (5x, 1mg/mouse/day; i.p.). *Fth*$^{Cdh5\Delta/\Delta}$ mice were used for experiments 4 weeks later.

qRT-PCR. Mice were sacrificed, perfused *in toto* with 10mL 1xPBS, and organs were harvested and snapped frozen in liquid nitrogen. RNA was isolated from mouse organs using TRIzol (Invitrogen Life Technologies) and the RNeasy Mini Kit (QIAGEN), from blood using the NucleoSpin® RNA Blood (Machery-Nagel) and from cell suspension using the NucleoSpin® RNA XS (Machery-Nagel). Total RNA was used to synthesize cDNA (Transcriptor First Strand cDNA Synthesis Kit, Roche) for qPCR with Power SYBR Green PCR master mix (Bio-Rad). Transcript number was calculated from the threshold cycle (Ct) of each gene with a $2^{-\Delta\Delta CT}$ method (relative number) and normalized to Acidic ribosomal phosphoprotein P0 (*Arbp0*). Allele deletion efficiency is represented as percentage of *Hmox1, Fth*, *Hsf1* or *Hif1*α mRNA expression in *Hmox1*$^{\Delta/\Delta}$, *Fth*$^{\Delta/\Delta}$, *Hsf1*$^{\Delta/\Delta}$ or *Hif1*$\alpha^{\Delta/\Delta}$ mice vs. *Hmox1*$^{fl/fl}$, *Fth*$^{fl/fl}$, *Hsf1*$^{fl/fl}$ or *Hif1*$\alpha^{fl/fl}$ mice, respectively. PCR primers include: *Hmox1 set 1* Fwd: 5'-AAGGAGGTACACATCCAAGCCGAG-3' and *Hmox1 set 1* Rev: 5'-

GATATGGTACAAGGAAGCCATCACCAG-3', *Hmox1 set 2* Fwd: 5'-TGACACCT GAGGTCAAGCAC-3' and *Hmox1 set 2* Rev: 5'-TCTCTGCAGGGGCAGTATCT-3'; *Arbp0* Fwd: 5'-CTTTGGGCATCACCACGAA-3' and *Arbp0* Rev: 5'-GCTGGC TCCCACCTTGTCT-3', *Fth* Fwd: 5'-CCATCAACCGCCAGATCAAC-3' and *Fth* Rev: 5'-GCCACATCATCTCGGTCAAA-3', *Slc40a1* Fwd: 5'-TGCCTTAGTTGTCCTTT GGG-3' and *Slc40a1* Rev: 5'- GTGGAGAGAGAGTGGCCAAG-3'; *Nqo1* Fwd: 5'-TTCTGTGGCTTCCAGGTCTT-3' and *Nqo1* Rev: 5'- AGGCTGCTTGGAGCAAAATA-3'; *Hsf1* Fwd: 5'-AGGCAGGAGCATAGATGAGA-3' and *Hsf1* Rev: 5'-AGGATGGAGTCAATGAAGGC-3', *Hif1*α Fwd: 5'-TCATCAGTTGCCACTTCCCCAC-3' and *Hif1*α Rev: 5'-CCGTCATCTGTTAGCACCATCAC-3'; *Lcn2* Fwd: 5'-ACTGAATG GGTGGTGAGTGTG-3'; *Lcn2* Rev: 5'-TATTCAGCAGAAAGGGGACG-3'. For analyses of gene expression, relative level of mRNA expression is represented as percentage over non-infected controls.

Disease assessment. *Plasmodium*-infected mice were monitored daily with the day of infection being considered as zero (D0). Rectal temperature was determined using a Rodent Thermometer BIO-TK8851 (Bioset). Number of RBC per mL of blood was quantified by flow cytometry on a CyAn ADP analyzer (Beckman Coulter) or on a FACSCalibur analyzer (BD Biosciences) using a known concentration of reference 10µm latex beads suspension (Coulter® CC Size Standard L10, Beckman Coulter), gating on RBC in blood samples, based on size and granularity and on bead population. Percentage of iRBCs (parasitemia) was determined by optical microscopy counting manually *Plasmodium* containing RBC in 4 fields of Giemsa-stained blood smears (1000x magnification). Parasite Density (Parasitemia x total RBC number) is expressed as iRBC/µL.

Heme quantification. Plasma (1µL) was diluted in H_2O (50µL) to which formic acid (150µL) was added. Heme absorbance was determined at λ_{405nm} and concentration calculated against serial dilutions of a hemin standard. Heme quantification in urine was performed as above, with the following modifications. Urine samples were diluted in H_2O to a total of 50µL, after which 150µL formic acid was added and absorbance measured at λ_{355nm} and λ_{405nm}. Because urine displays high background absorbance at λ_{355nm} and λ_{405nm}, sample absorbance at λ_{405nm} was corrected against $\lambda_{405nm}/\lambda_{355nm}$ absorbance ratio using the formula: $\lambda_{405nm}=\lambda_{405nm}x\ (\lambda_{405nm}/\lambda_{355nm})$. Heme

concentration was then calculated against serial dilutions of a hemin solution at known concentration, used as standards.

Histology and Immunofluorescence. Mice were sacrificed at the indicated time-points after *Plasmodium* infection, perfused *in toto* with ice-cold PBS and organs were harvested, fixed in 10% formalin, embedded in paraffin, sectioned (3μm) and stained with Hematoxylin & Eosin, or immunostained for Ho-1, Fth and Ggt1, as detailed bellow.

Quantification of bioavailable heme in plasma. Bioavailable heme was quantified essentially as described (17, 18). HEK293 cells (ATCC; $5x10^4$ cells/well in a 24 well plate) were grown overnight (DMEM, 10% FBS, 10000 U/mL penicillin, 10000 µg/mL streptomycin) and transfected (4h-6h, lipofectamin 2000; Invitrogen) with an expression vector encoding the HRP gene under the control of the EF-1α promoter (pEF5/FRT/V5-DEST-Golgi-HRP) in opti-MEM reduced serum (Gibco). Transfected cells were selected with hygromycin and plated in 96-well plates ($1.1x10^4$ cells/well). Cells were cultured in DMEM with 10% heme-depleted serum and 0.5 mM of succinylacetone (SA) to inhibit endogenous heme biosynthesis. 24h thereafter cells were exposed to hemin (calibration curve), plasma or urine in DMEM, supplemented with 10% heme-deplete serum and 0.5 mM SA (overnight) and HRP activity was assessed as a read-out of cellular heme content. Briefly, cells were lysed (20 mM HEPES pH 7.4, 150 mM NaCl, 0.5% Triton X-100, 2,5X protease inhibitor cocktail set; Calbiochem®) (Ice, 20 min.), centrifuged (4000 rpm, 4ºC, 30min.) and peroxidase activity was quantified in a 96 well plate using o-dianasidine and H_2O_2. Absorbance was measured in a microplate reader at λ_{440nm} (Victor3, PerkinElmer). Heme concentration in plasma and urine was determined based on the calibration curve performed with serial heme concentrations (0.0625-4 µM) and normalized to the total amount of protein as determined using Bradford Protein Assay (Bio-Rad).

ELISA. Mice were sacrificed at the indicated time-points after *Plasmodium* infection. Plasma was obtained from blood after 2 consecutive centrifugations (1600g, 5min, 4ºC). Lipocalin 2 concentration in plasma and urine were determined by ELISA (LEGEND MAX™ Mouse NGAL; Lipocalin-2 ELISA Kit with Pre-coated Plates, Biolegend), according to the manufacturer's instructions. Briefly, plasma and urine samples were diluted and incubated with plates pre-coated with a mouse anti-human NGAL monoclonal antibody (mAb) followed by incubation with a biotinylated anti-human NGAL mAb detection antibody. Detection was based on an Avidin-HRP chromogenic reaction, and absorbance was measured at λ_{450nm} and λ_{570nm} for background subtraction, in a Victor3 microplate reader (PerkinElmer). Cystatin C concentration in plasma was determined by ELISA (Mouse/Rat Cystatin C Quantikine ELISA Kit, R&D Systems), according to the manufacturer's instructions. Briefly, plasma samples were diluted and incubated with plates pre-coated with a polyclonal antibody specific for mouse/rat Cystatin C, followed by incubation with a HRP-conjugated mouse/rat Cystatin C-specific polyclonal antibody. Detection was based on an HRP-based chromogenic reaction, and absorbances were read at λ_{450nm} and λ_{570nm} for background subtraction, in a Victor3 microplate reader (PerkinElmer).

Histopathology. Whole sections from formalin fixed and Hematoxylin & Eosin stained tissues were analyzed and images were acquired with a DMLB2 microscope (Leica). Histology was analyzed by a pathologist (Pedro Faísca) at the Instituto Gulbenkian de Ciência Histopathology Unit.

Immunostaining. For antigen retrieval, slides containing 3μm-thick paraffin embedded tissue sections were placed in citrate buffer and heated to sub-boiling conditions for 6 min. After cooling down, slides were briefly washed in Tris-Buffered Saline with Tween-20 (TBST; Tris-base 20mM; NaCl 150mM; Tween 20 0,1%; pH 7.4) and permeabilized with 0.3% Triton (Sigma) in phosphate buffered saline (PBS). Slides were blocked (1h, RT) with blocking solution (goat serum; ThermoFisher Scientific; in TBST, 1:50) and incubated with primary antibodies (FTH1 D1D4; Cell Signaling, 1:100; HO1 EP1391Y, Abcam, 1:100; GGT1, Abcam, 1:200) in blocking solution (overnight; 4°C). Slides were quickly washed in TBST and incubated with secondary antibodies (Alexa Fluor® 568 Goat Anti-Rabbit and Alexa Fluor® 647 Goat Anti-Mouse, Life Technologies; 1:500) in blocking solution, (2 hr; RT), washed

first with TBST and then with PBS and mounted (Mowiol-Dabco; 10µg/mL 4',6-diamidino-2-phenylindole (DAPI)). Images were acquired on a commercial Leica High Content Screening microscope (Leica), based on Leica DMI6000 equipped with a Hamamatsu Flash Orca 4.0 sCMOS camera (Hamamatsu), using a 40x 1.3 NA HCX PLAN APO objective (Leica), DAPI + TRITC + fast filter wheels CY5 fluorescence filtersets and controlled with the Leica LAS X software. For whole kidney sections analysis, images were acquired on a commercial Nikon High Content Screening microscope, based on Nikon Ti equipped with a Andor Zyla 4.2 sCMOS camera, using the a 10x 0.45 NA objective, DAPI + TRITC + Cy5 fluorescence filtersets and controlled with the Nikon Elements software. Images were acquired using Large Image Acquisition setting of a defined area. Analysis was performed with ImageJ (Rasband, W.S., ImageJ, U. S. NIH, Bethesda, Maryland, USA, https://imagej.nih.gov/ij/, 1997-2014).

Western Blotting. For protein detection in human cultured RPTEC, cells were lysed (20 mM Tris-HCl, pH 7.5, 150 mM NaCl, 1 mM EDTA, 1% Triton X-100, 0.5% Nonidet, cOmplete™, Mini Protease Inhibitor Cocktail, Sigma). Total protein content was quantified using BCA protein assay (Pierce) and 20µg of total cell lysate was resolved (12.5% STDS-PAGE) and transferred to nitrocellulose membranes (Amersham). These were incubated with anti-Fth1 (clone D1D4; Cell Signaling; 1:1000) or HRP-conjugated anti-β-Actin (Santa Cruz Biotechnology, Inc., 1:500) rabbit polyclonal antibodies (overnight, 4ºC). Membranes were washed and the antibodies detected using peroxidase-conjugated goat anti-Rabbit IgG (Amersham) and goat anti-Mouse IgG (Amersham) polyclonal antibodies (1h; RT) and developed with ECL Western blotting Analysis System (Amersham).

For protein detection in mouse organs, these were harvested and lysed in 2X SDS page sample buffer (20% glycerol, 4% SDS, 100mM Tris pH6.8, 0.002% bromophenol blue,100mM DTT). DNA was digested with Benzonase nuclease (Merck Millipore). Proteins were heated (10min, 70ºC) and centrifuged (max speed, 10min). Supernatant was transferred into a new tube, loaded on a 12% SDS-PAGE and electrophoresed and electro transferred, essentially as described (19). Total protein content was quantified at Abs 280nm in Nanodrop 2000. Anti-Fth1 (clone D1D4; Cell Signaling; 1:1000) and anti-Gapdh (Sicgen, 1:4000) were incubated (overnight, 4ºC), detected using peroxidase-conjugated AffiniPure goat anti-Rabbit IgG (Jackson ImmunoResearch Laboratories, Inc.) and donkey anti-Goat IgG

(ThermoFischer Scientific) secondary antibodies (1h; RT) and developed with SuperSignal West Pico Chemiluminescent substrate (ThermoFisher Scientific) using Amersham Imager 680 (GE Healthcare), equipped with a Peltier cooled Fujifilm Super CCD. Densitometry analysis was performed with ImageJ (Rasband, W.S., ImageJ, U. S. NIH, Bethesda, Maryland, USA, https://imagej.nih.gov/ij/, 1997-2014), using images without saturated pixels.

For western blotting of HRP, proteins were collected from transfected HEK 293 cells in loading buffer (20 % v/v Glycerol, 0.2 M Tris-HCl, pH 6.8; 0.05% w/v Bromophenolblue), loaded (50 µg) onto 7% SDS-PAGE, transferred to polyvinyldifluoridine membrane and washed (1x, T-TBS). HRP activity was revealed immediately using peroxidase substrate (SuperSignal West Pico Chemiluminescent substrate) in a photoradiograph (Kodak Biomax Light Film; Eastman Kodak). Membrane was blocked (Protein-Free Blocking Buffer; 2-16h; RT) and probed with rabbit anti-HRP polyclonal Ab (Sigma, 1/2000; 1h, RT), washed (5x, T-TBS) and probed with Alakaline Phosphatase-conjugated goat anti-rabbit polyclonal Ab (Pierce; 1/5000; 1h, RT). Alakaline Phosphatase signal was detected using Lumi-Phos WB chemiluminescent Substract (Pierce) in a photoradiograph. Membranes were re-probed with anti-vinculin mouse mAb (1/3000, ON, 4ºC; Abcam) detected by HRP-conjugated goat anti-mouse IgG polyclonal Ab (1/2500; 1h, RT). HRP signal was detected as described above. All Abs were diluted in Protein-Free Blocking Buffer.

Cytotoxicity assay in Human RPTEC. Human RPTEC (ScienCell Research Laboratories) were cultured in DMEM (high glucose; Sigma-Aldrich Co.) supplemented with 10% FBS (Gibco, Thermo Fisher Scientific Inc.), Penicillin-Streptomycin and L-glutamine (Sigma-Aldrich Co.). Human RPTEC were grown in 96-well plates, washed twice with PBS and exposed to vehicle (HBSS medium without serum) or heme (5µM; 60 min) in HBSS (Sigma). After removal of heme, RPTEC were treated with vehicle or H_2O_2 in DMEM media (50µM; 4h). Cell viability was determined with MTT assay. Briefly, RPTEC were washed with PBS and 100 µL of 3-[4,5-Dimethylthiazol-2-yl]-2,5-diphenyl-tetrazolium bromide (0.5mg/mL) solution in HBSS was added. After a 4h incubation MTT solution was removed, formazan crystals were dissolved in 100µL of DMSO and optical density was measured at λ_{570nm}.

Intracellular ROS determination. ROS production was monitored using the 5- (and-6)-chloromethyl-2′,7′-dichlorodihydro-fluorescein di-acetate, acetyl ester (CM-H_2DCFDA) assay (Life Technologies). Human RPTEC were grown in 96-well plates washed with PBS and loaded with CM-H_2DCFDA (10mM, 30 min, in the dark). After washing thoroughly with PBS, cells were exposed to vehicle (HBSS medium without serum) or heme (5μM; 60 min). After removal of heme, cells were exposed to H_2O_2 in DMEM media (50μM) and fluorescence intensity was measured immediately applying λ_{488nm} excitation and λ_{533nm} emission wavelengths (every 30 minutes for 3h).

Flow cytometry. Mice were sacrificed, perfused *in toto* (10mL PBS) and kidneys were collected in RMPI, finely minced and digested with collagenase D (0.5 mg/mL, Roche) and type 1 deoxyribonuclease (10ug/mL, Roche) (1h, 37ºC) under agitation in RPMI medium supplemented with 10% heat-inactivated FCS (Invitrogen). Digested tissue was passed through 70- and 40-μm nylon meshes and red blood cells were lysed by addition of ammonium chloride (0,16M, 9 parts supplemented with 0,1M Tris HCL pH 7,5, 1 part; 5min, RT). To separate the leukocyte fraction, cells were resuspended in 36% Percoll, overlayed on 63% Percoll and spun (500g, RT; 25 min) without break and acceleration. Leukocytes were collected, washed (Ice cold PBS, 1X) and stained (20 min, 4°C) with fluorochrome-conjugated antibodies directed against: CD45 (Clone-APC-Cy7), TCR-beta (Clone-Bv421), CD4 (Clone-PeCy7), CD11b (M1/70, FITC), F4/80 (Clone-PeCy7), Cx3Cr1 (Clone-APC), Ly6G (Clone-Pe), and Ly6C (Clone-PercpCy5.5) (BD Biosciences, Franklin Lakes, NJ or eBioscience). FoxP3 and Ki67 intracellular staining was performed using the mouse FoxP3 staining Kit (eBiosciences) according to the manufacturer's instructions. For all experiments, cells were stained beforehand with Fc block (anti-CD16/CD32 produced in house) to prevent non-specific binding and with fixable Live-dead cells® dye (Invitrogen) to exclude dead cells. Cells were analyzed either on CyAn ADP (Beckman) or LSR Fortessa X-20 (BD Biosciences). FACS data was analyzed with FlowJo V10.

Endothelial cell isolation and culture. *Hmox1$^{fl/fl}$ and Hmox1$^{Tie2\Delta/\Delta}$* mice were sacrificed and perfused *in toto* (10mL PBS). The heart was collected into MCDB131 medium (Life Technologies), supplemented with 0.5% FBS, chopped into small pieces and digested with collagenase IA (Sigma-Aldrich co.; 2,2 U/mL, 45 min, 37%,

5% CO_2). Digested tissue was disrupted and passed through a 70μm cell strainer, washed in MCDB131 media and incubated (30 min. on ice) with rat anti-mouse CD31 antibody (BD Pharmigen™). Cell suspension was washed and incubated (15 min, on ice) with goat anti-rat IgG microbeads (MACS®; Miltenyi Biotec). $CD31^+$ cells were purified using a MACS LS column on a magnetic support (MACS®; Miltenyi Biotec). Isolated cells were seeded onto 0,2% gelatin-coated cell culture plates in MCDB131 medium supplemented with 20% FBS and allowed to grow for 2-3 days. After that initial growth was allowed in MCDB131 medium supplemented with 10% FBS until cells reached confluence for RNA extraction. A fraction of the cells was used for flow cytometry to confirm endothelial cell purity. Briefly, cells were incubated with anti-CD31-APC (BD Biosciences) and anti-CD105-PB (Biolegend) for 30 min on ice, in the dark. Acquisition was made in a CyAn ADP analyzer (Beckman Coulter), by gating on $CD31^+CD105^+$.

***E. coli* peritonitis.** Murine peritonitis was induced as previously described (20). Briefly, α-hemolytic *E. coli* strain CFT073 (serotype O6:K2:H1)(21, 22) was streaked out onto blood agar medium and cultured (overnight, 37°C). Six large colonies were inoculated in Luria-Bertani (LB) medium and cultured to mid-log phase for 1:45h, washed twice and suspended in saline. Age-matched mice were infected via intraperitoneal (i.p.) injection of 100 μL of *E. coli* suspension containing ~$5x10^4$ CFU. Serial dilutions of the inoculum suspension were plated on blood agar medium to assess viable CFU.

Statistical analysis. Statistically significant differences between two groups were assessed using a two-tailed unpaired Mann-Whitney *U* test or t-test. Where indicated, data with log-normal distribution (according to D'Agostino-Pearson test) was log-transformed prior to t-test. Comparisons between more than two groups were carried out by two-way ANOVA with Tukey's multiple-comparisons test. Survival curves are represented by Kaplan–Meier plots, and the survival difference between the groups was compared using the log-rank test. All statistical analyses were performed using GraphPad Prism 7 software. Differences were considered statistically significant at a P value <0.05. NS: Not significant, P >0.05; *: P<0.05, **: P<0.01; ***: P<0.001.

Disease trajectory analysis. Euclidean distances were computed between disease trajectories of different genotypes, as generated using % initial body weight and relative change (Δ) in initial body Temperature *vs.* Log (parasite density; Nr. of infected RBC/μL blood). Data were standardized to ensure that movement along each host variable axis is weighed similarly. For this, the minimum (*MIN*) and maximum (*MAX*) of each disease variable across all data sets was computed, and a standardized value was computed for each individual: x'= (x-MIN)/ (MAX-MIN), where x corresponds to the original value of the disease variable (day 0, before infection). Multidimensional Euclidean distances were computed between disease curves at any time point along the infection trajectory. For each data set, the Euclidean distances were compared between. *Hmox1*$^{Pepck\Delta/\Delta}$ *Hmox1*$^{R26\Delta/\Delta}$ or *Fth*$^{Pepck\Delta/\Delta}$ *vs.* control *Fth*$^{fl/fl}$ mice until the day before the first death. For all data sets, differences at specific time points were reported as uncorrected p-values from a Mann-Whitney *U* test.

Extended Author Contribution. MPS drove the study design and wrote the manuscript. S. Ramos contributed critically to study design, performed and/or contributed critically to all experiments, data analyzes and writing of the manuscript. ARC contributed to study design, performed Western blots for Ho-1 and Fth in different organs, immunostaining and bioavailable heme assays. BS assisted S Ramos. VJ performed *in vitro* experiments with human kidney cells. RG performed initial *in vivo* malaria experiments with AR. FB performed kidney leukocyte infiltration experiments. RM performed bacterial infections. PF performed and analyzed histopathology. DT contributed to the initial establishment and analyzes of disease trajectories. SC and S. Rebelo generated different mouse strains. LB monitored FTH expression. BB performed *in vivo* malaria experiments. TA monitored expression of NRF2-dependent genes. EG and CB developed and analyzed disease trajectories. SB, AZ and AA provided the original *Fth*$^{Pepck\Delta/\Delta}$ mice. All authors read and approved the manuscript.

Extended Acknowledgments

The authors thank all members of the Inflammation group (IGC) for insightful discussions and Ana Cunha for monitoring *Hmox1* deletion in dendritic cells. Fundação para a Ciência e Tecnologia grants PTDC/SAU-TOX/116627/2010, HMSP-ICT/0018/2011, LISBOA-01-0145-FEDER-029411 to MPS, SFRH/BPD/101608/2014 to ARC and SFRH/BD/51877/2012 to AR. TA was supported by Fundação Calouste Gulbenkian, grant 217/BD/17. BS, SC, LB, RG and S. Ramos were supported by European Community 7th Framework ERC-2011-AdG 294709-DAMAGECONTROL grant to MPS, VJ by National Research, Development and Innovation Office (NKFIH grant number: K116024), FB by Marie Skłodowska-Curie Research Fellowship 707998, RM by European Molecular Biology Organization (EMBO) long-term fellowship ALTF290-2017, AA National Institutes of Health (NIH) grants R01 DK059600 and P30 DK079337, SB by NIH grant K01 DK103931. We thank Sylvia Knapp (Laboratory of Infection Biology, Medical University Vienna) for providing E. coli hemolytic strains.

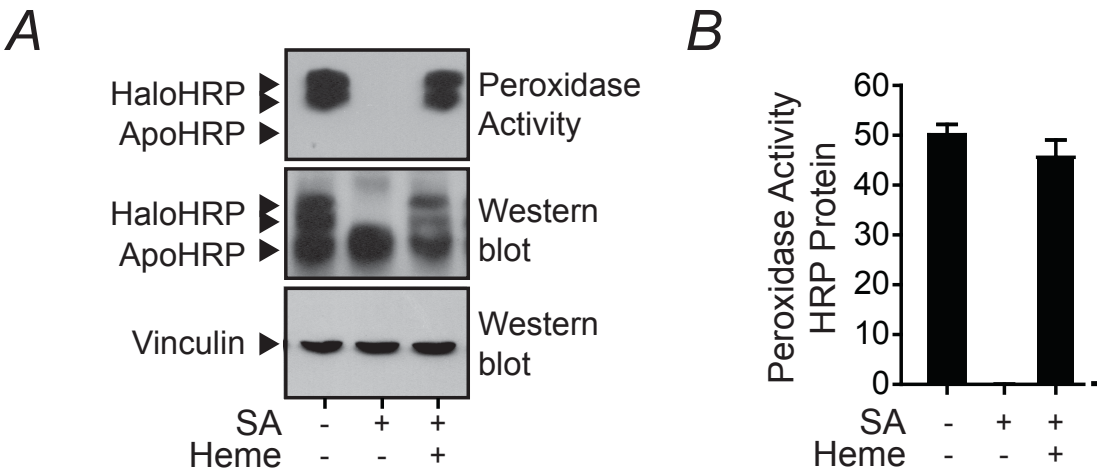

Fig. S1. **Bioavailable heme quantification assay.** ***A)*** Detection of bioavailable heme by peroxidase activity and western blot, in whole cell lysates from horseradish peroxidase (HRP)-reporter transfected HEK 293 cells. When indicated, cells were treated (+) or not (-) with the inhibitor of endogenous heme biosynthesis succinylacetone (SA) and exposed (+) or not (-) to exogenous heme (5μM). Upper panel illustrates HRP peroxidase activity, when the enzyme is reconstituted with heme (HaloHRP) and middle panel illustrates protein expression. ***B)*** Quantification of data obtained in one out of three independent experiments, shown as mean ± SD from three replicates.

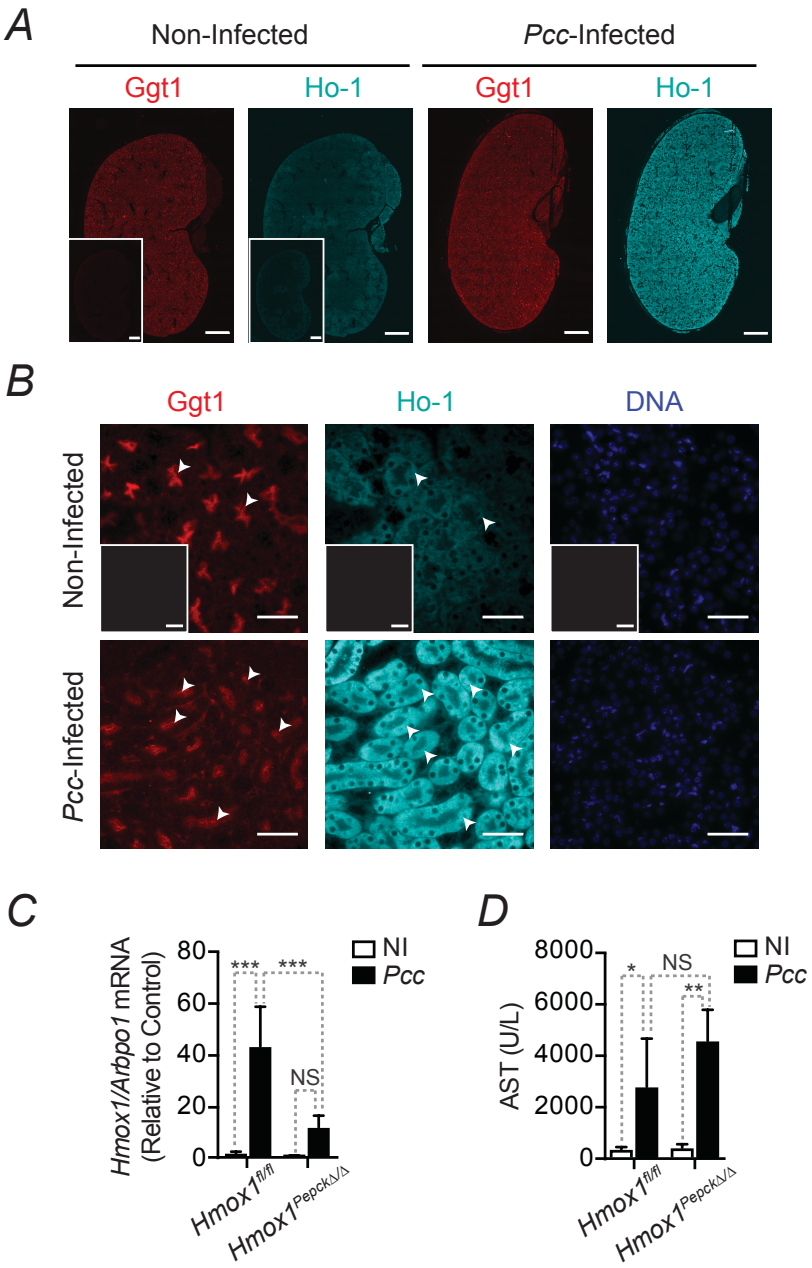

Fig. S2. **Induction of Ho-1 in response to *Pcc* infection.** ***A)*** Kidney Ho-1 immunostaining visualized by fluorescence microscopy in *Pcc*-infected and non-infected C57BL/6 mice, 7 days after infection. Ggt1: red, gamma glutamyl transferase 1 expression in RPTEC; Ho-1: cyan. Indented panels illustrate background staining with secondary antibody. Images are representative of 3 mice *per* group in one experiment. Scale bar = 1000µm. ***B***) Kidney HO-1 immunostaining as in (A). DNA: Blue, 4',6-diamidino-2-phenylindole (DAPI). Arrows highlight Ho-1 expression in Ggt1^{+} RPTEC. Images are representative of 5 random fields from 4-6 mice *per* group in one experiment. Scale bar = 50µm. ***C***) *Hmox1* mRNA normalized to *Arbp0* mRNA in kidneys of non-infected (NI) or 7 days after *Pcc* infection in *Hmox1*$^{fl/fl}$ (NI: N=5; *Pcc*: N=7) and *Hmox1*$^{PepcKΔ/Δ}$ (NI: N=4; Pcc: N=4) mice. Data represented as mean expression relative to NI *Hmox1*$^{fl/fl}$ mice ± SD, from 2 independent experiments with similar trend. ***D***) AST concentration in plasma of the same mice as in (*D*). Data represented as mean ± SD. P values in (C) and (D) determined using Two-way ANOVA with Tukey's multiple comparison test. NS: Not significant (P>0.05); *P<0.05, **P<0.01, ***P<0.001.

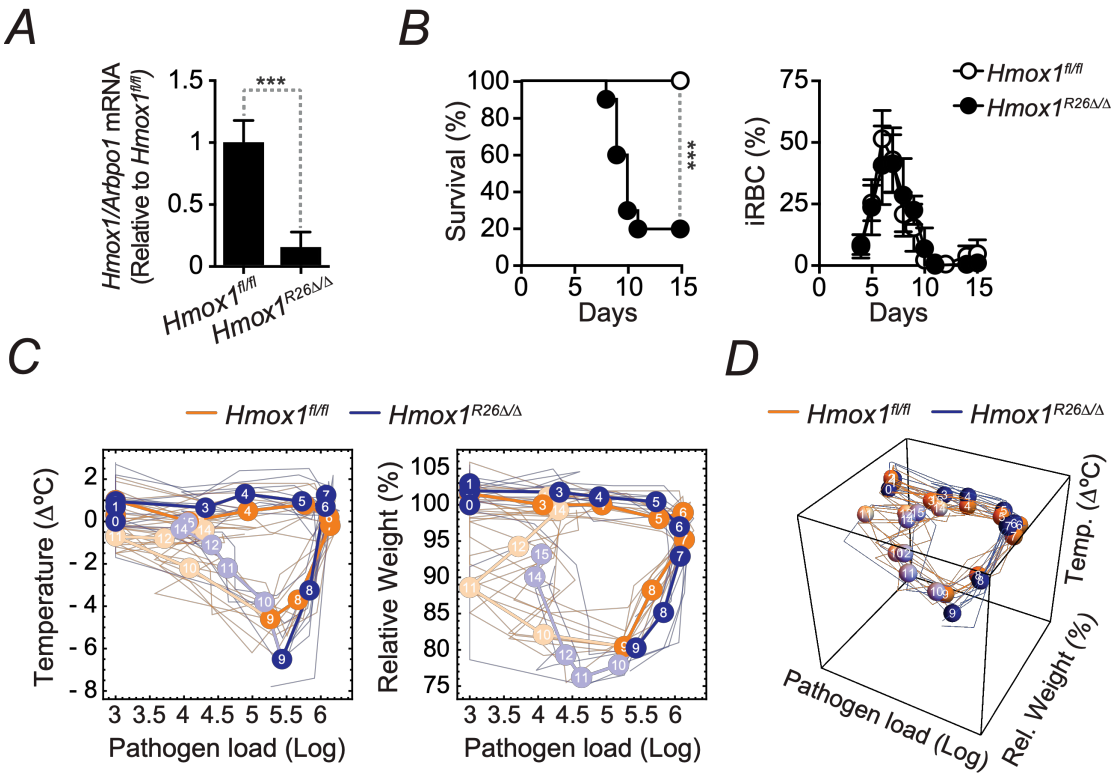

Fig. S3.* HO-1 expression is essential to establish disease tolerance to malaria.** ***A) Expression of *Hmox1* (mean ± SD) normalized to *Arbp0* mRNA in whole blood from *Hmox1*$^{fl/fl}$ (N=10) and *Hmox1*$^{R26\Delta/\Delta}$ (N=26) mice, represented as relative expression to *Hmox1*$^{fl/fl}$ mice. P values calculated using Mann-Whitney *U* test. ***: p<0.001. ***B)*** Survival and parasitemia (% iRBC; mean ± SD) of *Pcc*-infected *Hmox1*$^{fl/fl}$ (N=9) and *Hmox1*$^{R26\Delta/\Delta}$ (N=10) mice, from 2 independent experiments with similar trend. P value of survival determined using the Log-rank (Mantel-Cox) test. ***C)*** Individual disease trajectories of *Pcc*-infected *Hmox1*$^{fl/fl}$ (N=9) and *Hmox1*$^{R26\Delta/\Delta}$ (N=8) mice, from 2 independent experiments with similar trend. Circles represent median of disease trajectories for each genotype and numbers inside circles indicate days after the infection (Day 0). Disease trajectories in darker color indicate days before onset of mortality in *Hmox1*$^{R26\Delta/\Delta}$ mice. ***D)*** 3D plot of disease trajectories from same mice as C*)*. Statistical differences between genotypes became significant on day 7 (p=0.0003; Mann-Whitney *U* test), before onset of mortality of *Hmox1*$^{R26\Delta/\Delta}$ mice.

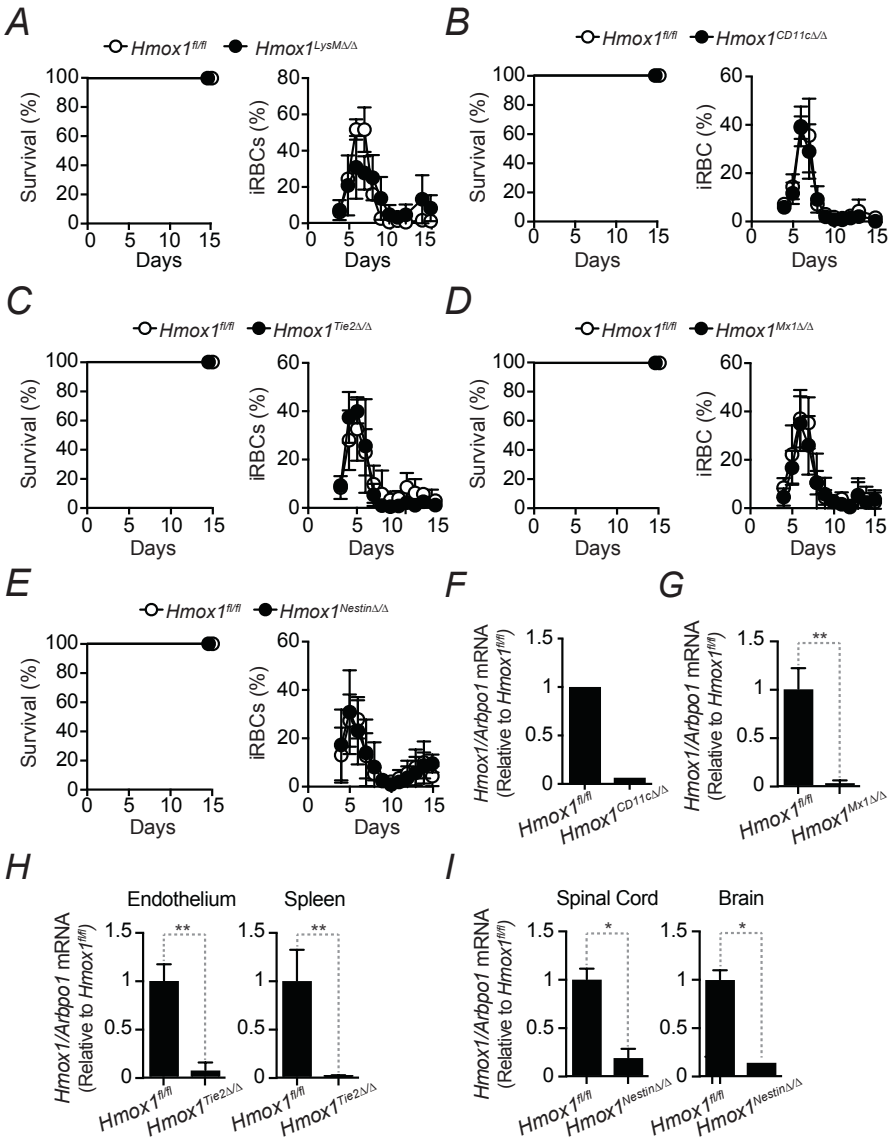

Fig. S4. **HO-1 expression in cell compartments other than RPTEC is not required to establish disease tolerance to malaria.** Survival and parasitemias (% iRBC; mean ± SD) of *Pcc*-infected ***A)*** $Hmox1^{LysM\Delta/\Delta}$ (N=6) and $Hmox1^{fl/fl}$ (N=4) mice, from 3 independent experiments with similar trend; ***B)*** $Hmox1^{CD11c\Delta/\Delta}$ (N=6) and $Hmox1^{fl/fl}$ (N=6) mice, from one experiment; ***C)*** $Hmox1^{Tie2\Delta/\Delta}$ (N=9) and $Hmox1^{fl/fl}$ (N=15) mice, from 2 independent experiments with similar trend; ***D)*** $Hmox1^{Mx1\Delta/\Delta}$ (N=10) and $Hmox1^{fl/fl}$ (N=8) mice, from 2 independent experiments, with similar trend; and ***E)*** *Pcc*-infected $Hmox1^{Nestin\Delta/\Delta}$ (N=9) and $Hmox1^{fl/fl}$ (N=14) mice, from 2 independent experiments with similar trend. Expression of *Hmox1* mRNA (mean ± SD) normalized to *Arbp0* mRNA in ***F)*** FACS-sorted $CD11c^{+}$ cells from $Hmox1^{fl/fl}$ (N=1) and $Hmox1^{CD11c\Delta/\Delta}$ (N=1) mice, ***G)*** whole blood from $Hmox1^{fl/fl}$ (N=4) and $Hmox1^{Mx1\Delta/\Delta}$ (N=8) mice, ***H)*** Purified $CD31^{+}$ endothelial cells and whole spleens from $Hmox1^{fl/fl}$ (N=3-5) and $Hmox1^{Tie2\Delta/\Delta}$ (N=3-5) mice, ***I)*** brain and spinal cord from $Hmox1^{fl/fl}$ (N=4) and $Hmox1^{Nestin\Delta/\Delta}$ (N=4) mice. Expression of mRNA in *F-I)* was quantified by qRT-PCR and is represented as relative expression to $Hmox1^{fl/fl}$ mice, from 1-3 independent experiments. P values were calculated using Mann-Whitney *U* test. *P<0.05, **P<0.01.

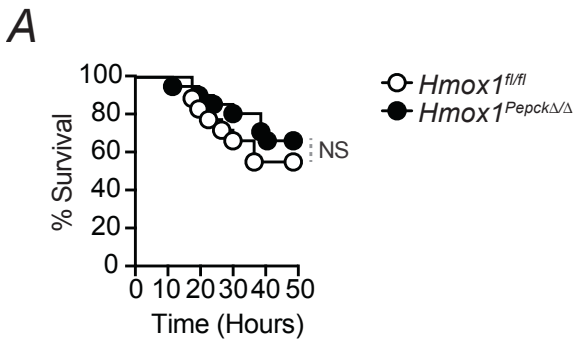

Fig. S5. Hmox1* deletion in RPTEC does not render mice susceptible to hemolytic bacterial infection.** ***A) Survival of *Hmox1*$^{fl/fl}$ (N=18) and *Hmox1*$^{Pepck\Delta/\Delta}$ (N=21) mice infected (i.p.) with the α-hemolytic E. coli strain CFT073 (serotype O6:K2:H1). Data pooled from 3 independent experiments with similar trend. P values of survival curve determined with Log-rank (Mantel-Cox) test. NS: Not significant ($p>0.05$).

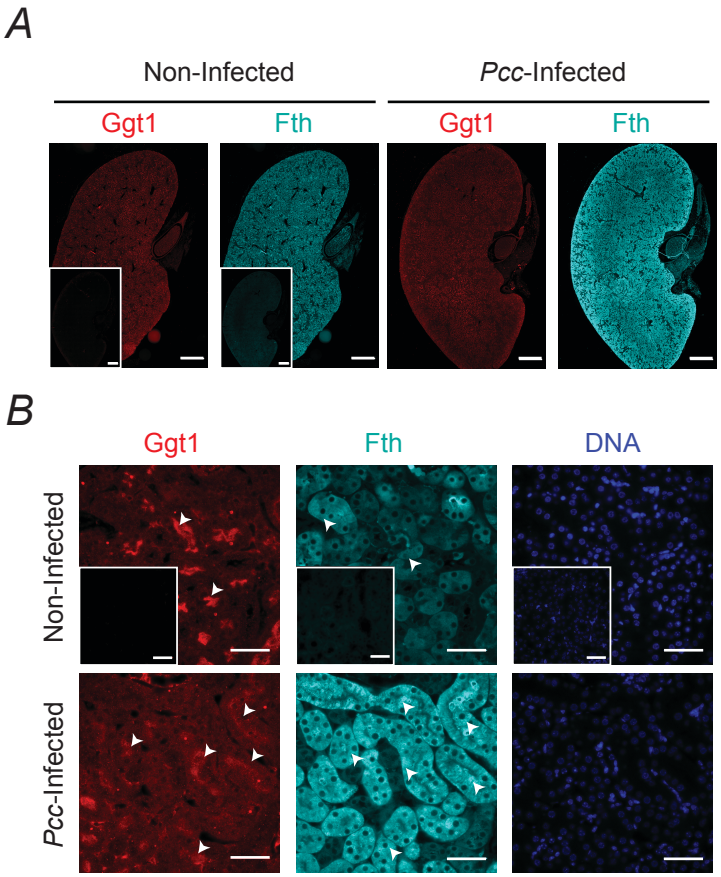

Fig. S6*. Induction of FTH expression in RPTEC in response to *Pcc* infection. *A) Kidney Fth immunostaining visualized by fluorescence microscopy in Pcc-infected and non-infected C57BL/6 mice, 7 days after infection. Ggt1: red, gamma glutamyl transferase 1 (RPTEC); Fth: cyan. Indented panels illustrate background staining with secondary antibody. Images are representative of 3 mice *per* group, in one experiment. Scale bar = 1000µm. ***B***) Kidney Fth immunostaining as in (A). DNA: Blue, 4',6-diamidino-2-phenylindole (DAPI). Arrows highlight Fth expression in $Ggt1^{+}$ RPTEC. Images are representative of 5 random fields from 4-6 mice *per* group, in one experiment. Scale bar = 50µm.

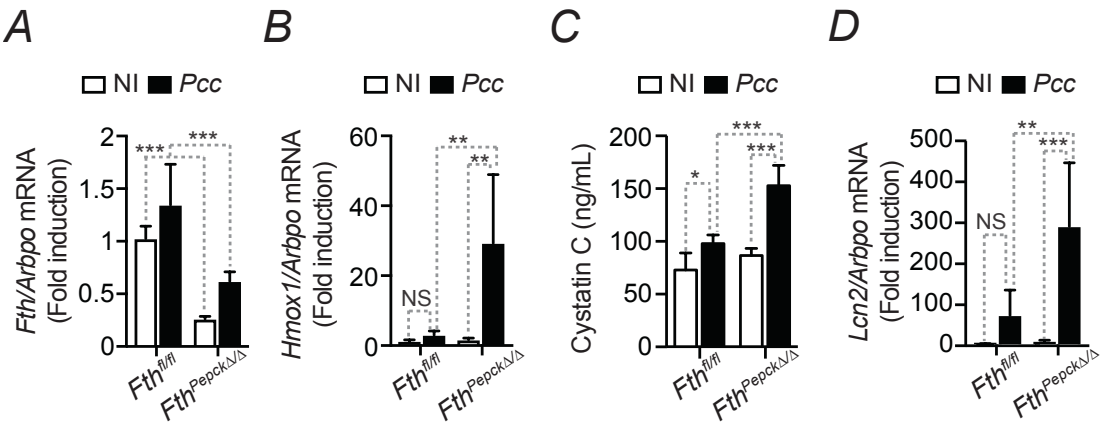

Fig. S7. **FTH expression in RPTEC protects mice from AKI and regulates Fe metabolism in kidneys.** Expression of ***A)*** *Fth* and ***B)*** *Hmox1* normalized to *Arbp0* mRNA in the kidneys of non-infected (NI) or 9 days after *Pcc* infection in $Fth^{fl/fl}$ (NI: N=6; *Pcc*: N=5) and $Fth^{PepcKΔ/Δ}$ (NI: N=4; *Pcc*: N=6) mice. Data represented as mean expression relative to NI $Fth^{fl/fl}$ mice ± SD, from 3 independent experiments with similar trend. ***C)*** Cystatin C concentration in the plasma of non-infected (NI) or 7 days after *Pcc* infection in $Fth^{fl/fl}$ (NI: N=3; *Pcc*: N=5) and $Fth^{PepcKΔ/Δ}$ (NI: N=4; *Pcc*: N=5) mice. Data represented as mean ± SD, from 2 independent experiments, with similar trend. ***D)*** *Lcn2* mRNA expression in the same kidneys as (*A*). Data calculated and represented as in (*A,B*). P values determined using two-way ANOVA with Tukey's multiple comparison tests. NS: Not significant (P>0.05); *P<0.05, **P<0.01; ***P<0.001.

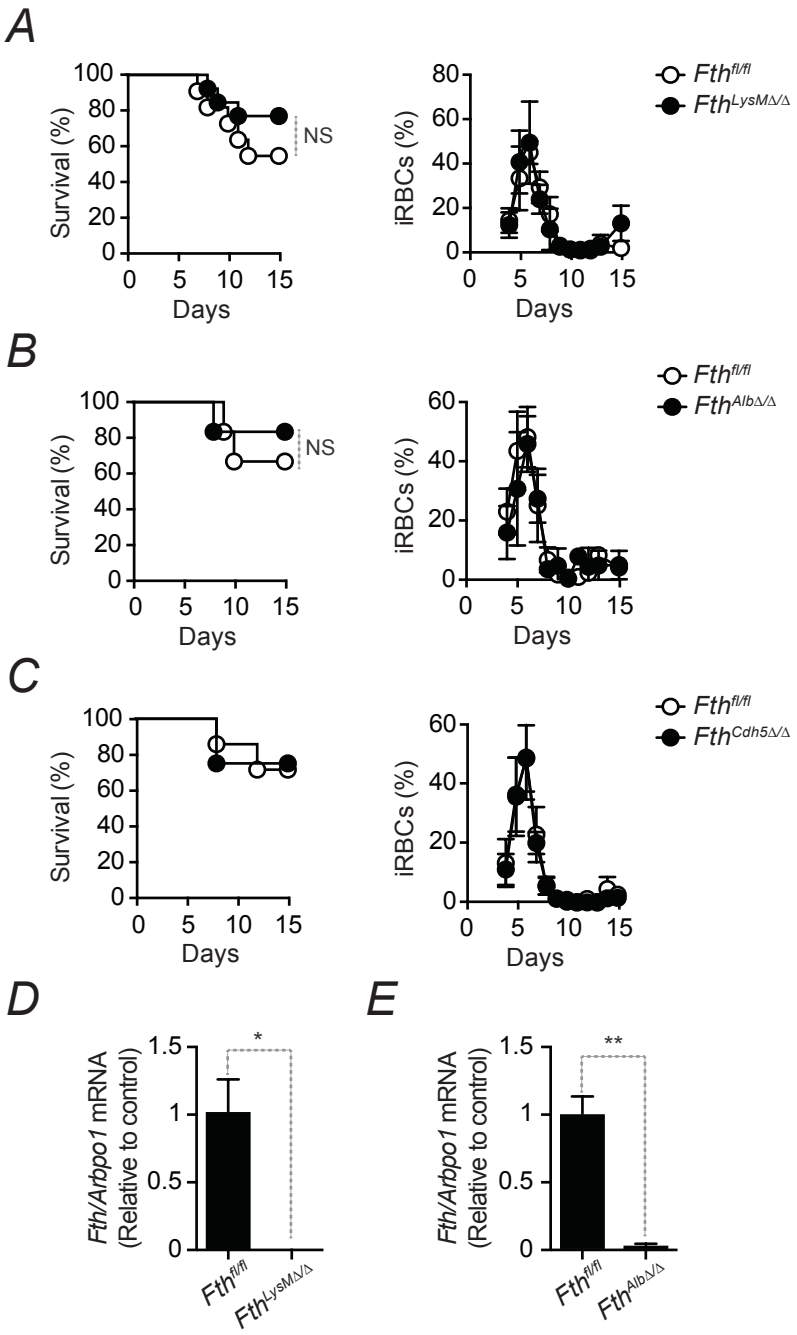

Fig. S8. **FTH expression in cell compartments other than RPTEC is not required to establish disease tolerance to *Pcc* infection.** Survival and percentage of infected red blood cells (iRBC) in *Pcc*-infected ***A)*** $Fth^{fl/fl}$ (N=11) and $Fth^{LysM\Delta/\Delta}$ (N=13) mice, from 3 independent experiments with similar trend, ***B)*** $Fth^{fl/fl}$ (N=6) and $Fth^{Alb\Delta/\Delta}$ (N=6) mice, from 3 independent experiments with similar trend, ***C)*** $Fth^{fl/fl}$ (N=7) and $Fth^{Cdh5\Delta/\Delta}$ (N=8) mice, from 2 independent experiments with similar trend. Statistical significance of survival curves was determined using the Log-rank (Mantel-Cox) test. Data for percentage of iRBC is represented as mean ± SD. *Fth* mRNA normalized to *Arbp0* mRNA expression, quantified by qRT-PCR, in ***D)*** bone marrow-derived macrophages from $Fth^{fl/fl}$ (N=4) and $Fth^{LysM\Delta/\Delta}$ (N=4) mice, ***E)*** whole livers from $Fth^{fl/fl}$ (N=5) and $Fth^{Alb\Delta/\Delta}$ (N=6) mice. Data is represented as relative expression to $Fth^{fl/fl}$ mice ± SD and is derived from 2 independent experiments. P values were calculated using Mann-Whitney *U* test. *P<0.05, **P<0.01. NS: Not significant (P>0.05).

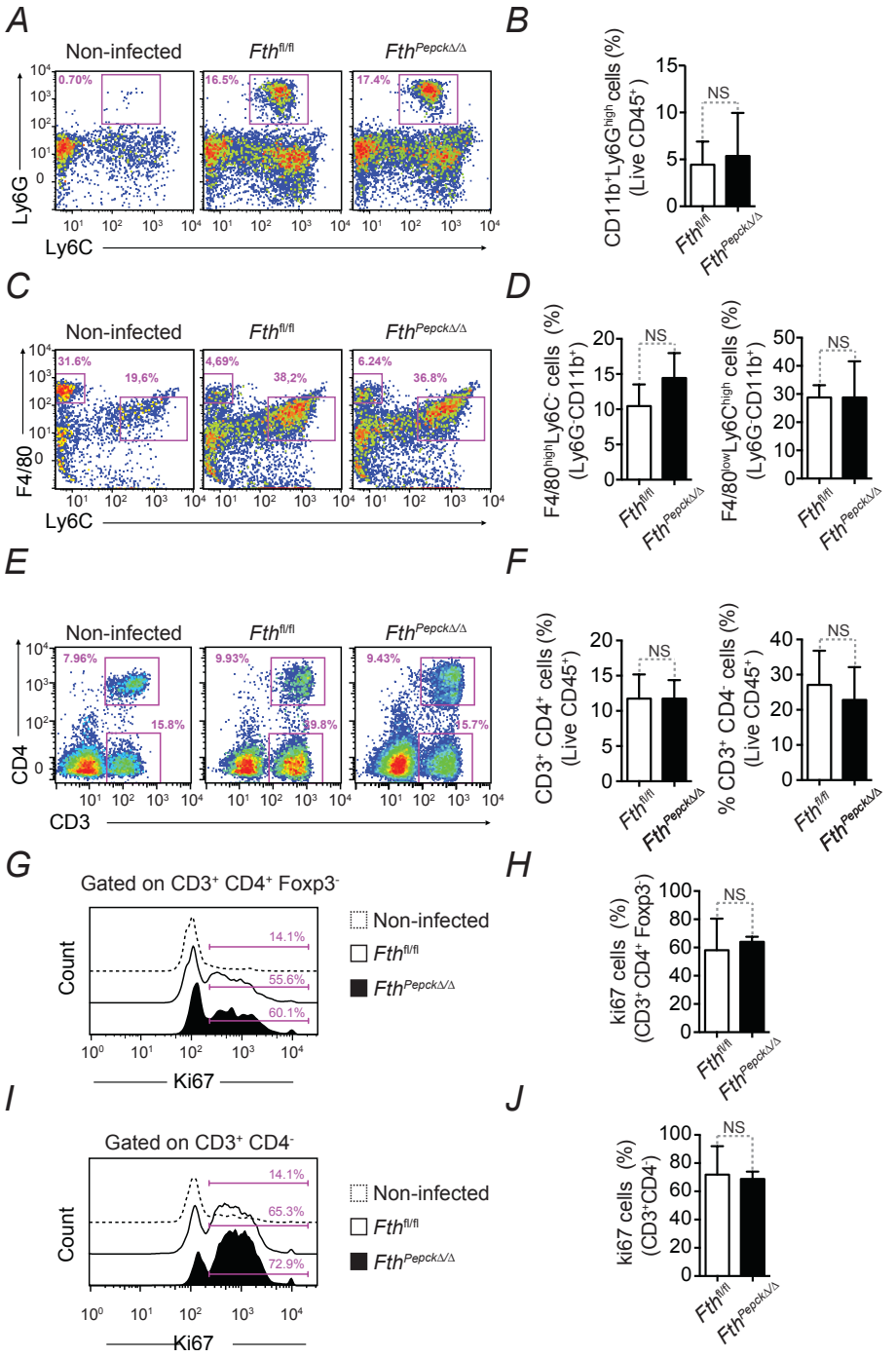

Fig. S9. **FTH expression in RPTEC does not influence kidney leukocyte infiltration in response to *Pcc* infection**. Quantification of renal ***A-B)*** $CD11b^{+}Ly6G^{high}$ neutrophils, ***C-D)*** $CD11b^{+}Ly6G^{-}F4/80^{high}Ly6C^{-}$ resident macrophages and $CD11b^{+}Ly6G^{-}F4/80^{low}Ly6C^{high}$ inflammatory monocytes, ***E-F)*** total $CD4^{+}$ and $CD4^{-}$ T cells and ***G-J)*** proliferating $Ki67^{+}CD4^{+}$ and $Ki67^{+}CD4^{-}$ T cells 9 days after *Pcc* infection in $Fth^{PepcKΔ/Δ}$ and $Fth^{fl/fl}$ mice (N=3-6). Data pooled from 2 independent experiments with similar trend. P values determined using Mann-Whitney *U* test. NS: Not significant (P>0.05).

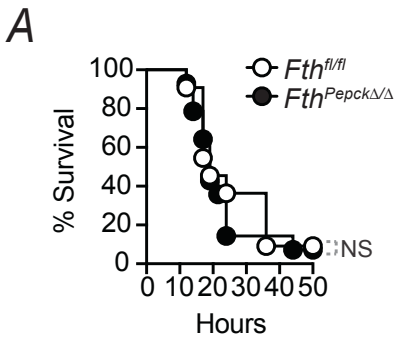

Fig. S10. **FTH expression in RPTEC does not prevent mortality from hemolytic bacterial infection.** ***A)*** Survival of *Fth*$^{fl/fl}$ (N=11) and *Fth*$^{PepckΔ/Δ}$ (N=14) mice infected (i.p.) with the α-hemolytic *E. coli* strain CFT073 (serotype O6:K2:H1). Data from one experiment. NS: Not significant (P>0.05).

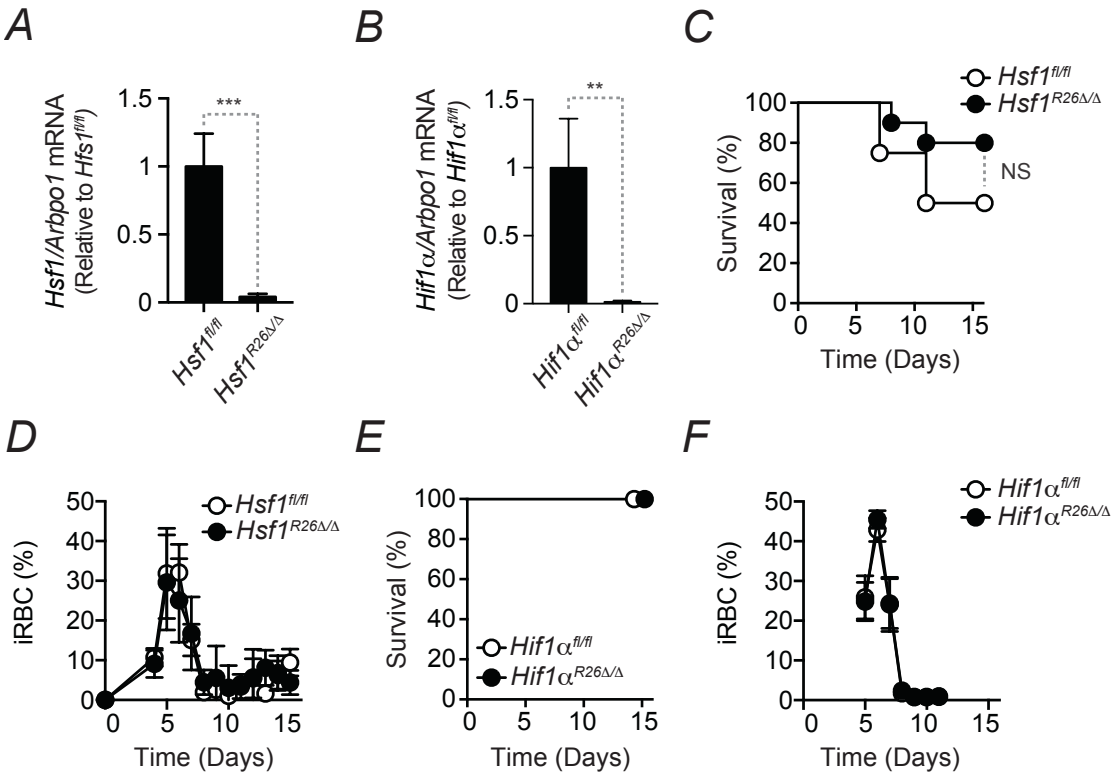

Fig. S11*. HSF1 or HIF1α are not essential *per se* to establish disease tolerance to *Pcc* infection.** ***A) *Hsf1* mRNA quantified by qRT-PCR in whole blood from $Hsf1^{fl/fl}$ (N=3) or $Hsf1^{R26\Delta/\Delta}$ (N=4) mice. Data represented as ratio of *Hsf1* to *Arbp0* mRNA (mean ± SD), relative to $Hsf1^{fl/fl}$ mice in one out of 6 representative experiments. ***B)*** Quantification of *Hif1α* mRNA quantified by qRT-PCR in whole blood from $Hif1\alpha^{fl/fl}$ (N=3) or $Hif1\alpha^{R26\Delta/\Delta}$ (N=4) mice. Data represented as ratio of *Hif1α* to *Arbp0* mRNA (mean ± SD), relative to $Hif1\alpha^{fl/fl}$ mice in one experiment. ***C)*** Survival and ***D)*** Percentage of iRBC (mean ± SD) of *Pcc*-infected $Hsf1^{fl/fl}$ (N=4) and $Hsf1^{R26\Delta/\Delta}$ (N=10) mice in one experiment. ***E)*** Survival and ***F)*** Percentage of iRBC (mean ± SD) of *Pcc*-infected $Hif1\alpha^{fl/fl}$ (N=7) and $Hif1\alpha^{R26\Delta/\Delta}$ (N=4) mice in one experiment. P values in (A) and (B) were calculated using Unpaired t test; in (C) and (E) using Log-rank (Mantel-Cox) test. NS: Not significant (P>0.05); **P<0.01, ***P<0.001.

Table 1. Complete Blood Count of Pcc-infected and non-infected *Hmox1*$^{lox/lox}$ and *Hmox1*$^{PepckΔ/Δ}$

	Non-Infected		*Pcc*-Infected	
	Hmox1$^{lox/lox}$	*Hmox1*$^{PepckΔ/Δ}$	*Hmox1*$^{lox/lox}$	*Hmox1*$^{PepckΔ/Δ}$
N	*7*	*4*	*7*	*3*
Erythrocytes (x10^6/μL)	10,03 ± 0,44	10,08 ± 0,74	2,51 ± 0,53[a]	2,33 ± 0,27[b]
Hb (g/dL)	14,64 ± 0,43	14,63 ± 1,3	3,70 ± 0,57[a]	3,37 ± 0,40[b]
Hematocrit (%)	53,44 ± 1,49	53,5 ± 3,67	13,45 ± 2,69[a]	12,27 ± 1,17[b]
MCV (μL)	53,26 ± 1,01	53,13 ± 0,79	53,65 ± 1,32	52,67 ± 1,24
MCH (pg)	14,59 ± 0,28	14,50 ± 0,22	14,87 ± 1,18	14,50 ± 0,56
MCHC (g/dL)	27,37 ± 0,24	27,33 ± 0,54	27,67 ± 2,07	27,47 ± 1,34
RDW (%)	13,44 ± 0,57	14,08 ± 0,98	24,38 ± 3,19[a]	22,97 ± 1,72[b]
Leukocytes (x10^3/μL)	9,11 ± 1,20	8,58 ± 3,17	22,65 ± 8,221[a]	22,87 ± 4,67[b]
Lymphocytes (x10^3/μL)	6,90 ± 1,53	6,18 ± 3,31	13,62 ± 4,37[a]	11,97 ± 4,27
Monocytes (x10^3/μL)	1,00 ± 0,37	0,83 ± 0,30	1,92 ± 1,94	0,57 ± 0,12
Neutrophils (x10^3/μL)	0,81 ± 0,30	1,28 ± 0,50	5,52 ± 3,24[a]	8,70 ± 1,47[b]
Eosinophils (x10^3/μL)	0,24 ± 0,05	0,23 ± 0,13	0,28 ± 0,33	0,47 ± 0,12
Basophils (x10^3/μL)	0,17 ± 0,05	0,10 ± 0,08	0,38 ± 0,37	0,13 ± 0,06
Platelets (x10^3/μL)	1377 ± 168,3	1475 ± 362,4	972 ± 418,6	1004 ± 228,3
Reticulocytes (x10^3/μL)	285 ± 48,05	343 ± 108,61	270 ± 58,18	371 ± 108,67
Total Bilirubin (mg/dL)	0,28 ± 0,03	0,28 ± 0,11	0,75 ± 0,25[a]	0,61 ± 0,04[b]
Direct Bilirubin (mg/dL)	0,14 ± 0,02	0,14 ± 0,05	0,37 ± 0,09[a]	0,43 ± 0,04[b]
Indirect Bilirubin (mg/dL)	0,14 ± 0,02	0,14 ± 0,07	0,38 ± 0,16[a]	0,18 ± 0,05[c]

[a] Statistically different from NI *Hmox1*$^{lox/lox}$
[b] Statistically different from NI *Hmox1*$^{PepckΔ/Δ}$
[c] Statistically different from *Pcc*-infected *Hmox1*$^{lox/lox}$
Statistical significance determined by 2 Way ANOVA with multiple comparisons by Tukey's test

References

1. Itoh K*, et al.* (1997) An Nrf2/small Maf heterodimer mediates the induction of phase II detoxifying enzyme genes through antioxidant response elements. *Biochem Biophys Res Commun* 236(2):313-322.
2. Higgins DF*, et al.* (2007) Hypoxia promotes fibrogenesis in vivo via HIF-1 stimulation of epithelial-to-mesenchymal transition. *J Clin Invest* 117(12):3810-3820.
3. Rankin EB, Tomaszewski JE, & Haase VH (2006) Renal cyst development in mice with conditional inactivation of the von Hippel-Lindau tumor suppressor. *Cancer Res* 66(5):2576-2583.
4. Mamiya T*, et al.* (2008) Hepatocyte-specific deletion of heme oxygenase-1 disrupts redox homeostasis in basal and oxidative environments. *Tohoku J Exp Med* 216(4):331-339.
5. Darshan D, Vanoaica L, Richman L, Beermann F, & Kuhn LC (2009) Conditional deletion of ferritin H in mice induces loss of iron storage and liver damage. *Hepatology* 50(3):852-860.
6. Kuhn R, Schwenk F, Aguet M, & Rajewsky K (1995) Inducible gene targeting in mice. *Science* 269(5229):1427-1429.
7. Ventura A*, et al.* (2007) Restoration of p53 function leads to tumour regression in vivo. *Nature* 445(7128):661-665.
8. Le Masson F*, et al.* (2011) Identification of heat shock factor 1 molecular and cellular targets during embryonic and adult female meiosis. *Mol Cell Biol* 31(16):3410-3423.
9. Ryan HE*, et al.* (2000) Hypoxia-inducible factor-1alpha is a positive factor in solid tumor growth. *Cancer Res* 60(15):4010-4015.
10. Parada E*, et al.* (2013) The Microglial alpha7-Acetylcholine Nicotinic Receptor Is a Key Element in Promoting Neuroprotection by Inducing Heme Oxygenase-1 via Nuclear Factor Erythroid-2-Related Factor 2. *Antioxid Redox Signal*.
11. Caton ML, Smith-Raska MR, & Reizis B (2007) Notch-RBP-J signaling controls the homeostasis of CD8- dendritic cells in the spleen. *J Exp Med* 204(7):1653-1664.
12. Postic C*, et al.* (1999) Dual roles for glucokinase in glucose homeostasis as determined by liver and pancreatic beta cell-specific gene knock-outs using Cre recombinase. *J Biol Chem* 274(1):305-315.
13. Weis S*, et al.* (2017) Metabolic adaptation establishes disease tolerance to sepsis. *Cell* 169:1263–1275.
14. Kisanuki YY*, et al.* (2001) Tie2-Cre transgenic mice: a new model for endothelial cell-lineage analysis in vivo. *Dev Biol* 230(2):230-242.
15. Buguet A, Vincendeau P, Bouteille B, Burlet S, & Cespuglio R (1999) Nitric oxide in murine malaria: divergent roles in blood and brain suggested by voltametric measures. *Trans R Soc Trop Med Hyg* 93(6):663-664.
16. Wang Y*, et al.* (2010) Ephrin-B2 controls VEGF-induced angiogenesis and lymphangiogenesis. *Nature* 465(7297):483-486.
17. Gouveia Z*, et al.* (2017) Characterization of plasma labile heme in hemolytic conditions. *FEBS J* 284(19):3278-3301.
18. Yuan X*, et al.* (2016) Regulation of intracellular heme trafficking revealed by subcellular reporters. *Proc Natl Acad Sci U S A* 113(35):E5144-5152.
19. Pamplona A*, et al.* (2007) Heme oxygenase-1 and carbon monoxide suppress the pathogenesis of experimental cerebral malaria. *Nat Med* 13(6):703-710.
20. Martins R*, et al.* (2016) Heme drives hemolysis-induced susceptibility to infection via disruption of phagocyte functions. *Nat Immunol* 17(12):1361-1372.

21. Welch RA*, et al.* (2002) Extensive mosaic structure revealed by the complete genome sequence of uropathogenic Escherichia coli. *Proc Natl Acad Sci U S A* 99(26):17020-17024.
22. Mobley HL*, et al.* (1990) Pyelonephritogenic Escherichia coli and killing of cultured human renal proximal tubular epithelial cells: role of hemolysin in some strains. *Infect Immun* 58(5):1281-1289.